PEGylated Human Plasma Fibronectin is Proteolytically Stable, Supports Cell Adhesion, Cell Migration, Focal Adhesion Assembly, and Fibronectin Fibrillogenesis

Chen Zhang, Sogol Hekmatfar, Anand Ramanathan, and Nancy W. Karuri
Dept. of Chemical and Biological Engineering, Illinois Institute of Technology, Chicago, IL 60616

DOI 10.1002/btpr.1689
Published online March 6, 2013 in Wiley Online Library (wileyonlinelibrary.com)

Delayed wound healing in many chronic wounds has been linked to the degradation of fibronectin (FN) by abnormally high protease levels. We sought to develop a proteolytically stable and functionally active form of FN. For this purpose, we conjugated 3.35 kDa polyethylene glycol diacrylate (PEGDA) to human plasma fibronectin (HPFN). Conjugation of PEGDA to HPFN or HPFN PEGylation was characterized by an increase of approximately 16 kDa in the average molecular weight of PEGylated HPFN compared to native HPFN in SDS-PAGE gels. PEGylated HPFN was more resistant to α chymotrypsin or neutrophil elastase digestion than native HPFN: after 30 min incubation with α chymotrypsin, 56 and 90% of native and PEGylated HPFN respectively remained intact. PEGylated HPFN and native HPFN supported NIH 3T3 mouse fibroblast adhesion and spreading, migration and focal adhesion formation in a similar manner. Fluorescence microscopy showed that both native and PEGylated HPFN in the culture media were assembled into extracellular matrix (ECM) fibrils. Interestingly, when coated on surfaces, native but not PEGylated HPFN was assembled into the ECM of fibroblasts. The proteolytically stable PEGylated HPFN developed herein could be used to replenish FN levels in the chronic wound bed and promote tissue repair. © 2013 American Institute of Chemical Engineers *Biotechnol. Prog.*, 29: 493–504, 2013
Keywords: fibronectin, polyethylene glycol, proteolysis, adhesion, spreading, migration, focal adhesion, fibrillogenesis, chymotrypsin, neutrophil elastase

Introduction

Hard-to-heal wounds or chronic wounds afflict 3–6 million Americans and their treatment is estimated to cost the US tax payer 3 billion dollars annually.[1] Chronic wounds have an abnormally higher immune cell level than normal healing wounds: the level of proteases such as neutrophil elastase is higher in chronic wound beds than in wounds that heal normally.[2–5] The high level of proteases leads to degradation of fibronectin (FN) in the wound bed.[2,6–9] FN is a key component of the provisional extracellular matrix (ECM), which is a scaffold for tissue repair. It attracts and binds different molecules and cells and thereby supports biological responses associated with wound healing. These include fibroblast migration into the wound bed, adhesion to the provisional ECM, proliferation and ECM assembly and remodeling.[10,11] Furthermore, proteolytic FN fragments stimulate the production of more proteases by immune cells,[12–14] leading to a destructive cycle of inflammation and FN degradation in chronic wounds. Stabilizing FN may be key to promoting tissue repair in chronic wounds.

FN is a dimer with a molecular weight of 230–270 kDa. It is composed of repeating units or repeats, that are classified as types I, II, and III (Figure 1A). These repeats harbor intermolecular binding sites that mediate cell adhesion, migration, proliferation, and ECM assembly at the wound site.[15] The cell-binding domain of FN found in the ninth and tenth type III repeats, $III_{9–10}$, supports interactions with cells.[16,17] In the wound context, FN has two physical forms: a secreted soluble form in wound exudates and blood plasma, and a fibrillar form in the provisional ECM that is assembled by fibroblasts.[18] The fibrillar form of FN comes from intermolecular FN-FN interactions in the type III repeats (Figure 1A). A strategy to stabilize FN needs to take into account these multiple functional sites in FN.

In this study, we have developed a conjugate of polyethylene glycol (PEG) and human plasma FN (HPFN) that is proteolytically stable and biologically active. Protein PEGylation has been used in the pharmaceutical industry to stabilize protein therapeutics.[19–21] HPFN is incorporated into the provisional ECM in the wound bed after injury and is an integral part of the scaffold needed for tissue repair.[22–24] HPFN was purified from blood plasma then conjugated to PEG Diacrylate (PEGDA) at reduced cysteine residues. Cysteine residues are concentrated in the 70 kDa amino-terminal of HPFN[25] whereas the type III repeats, which make up two thirds of FN by weight have only two cysteines.[26] Type III

Additional Supporting Information may be found in the online version of this article.

Corresponding concerning this article should be addressed to N. W. Karuri at nkaruri1@iit.edu.

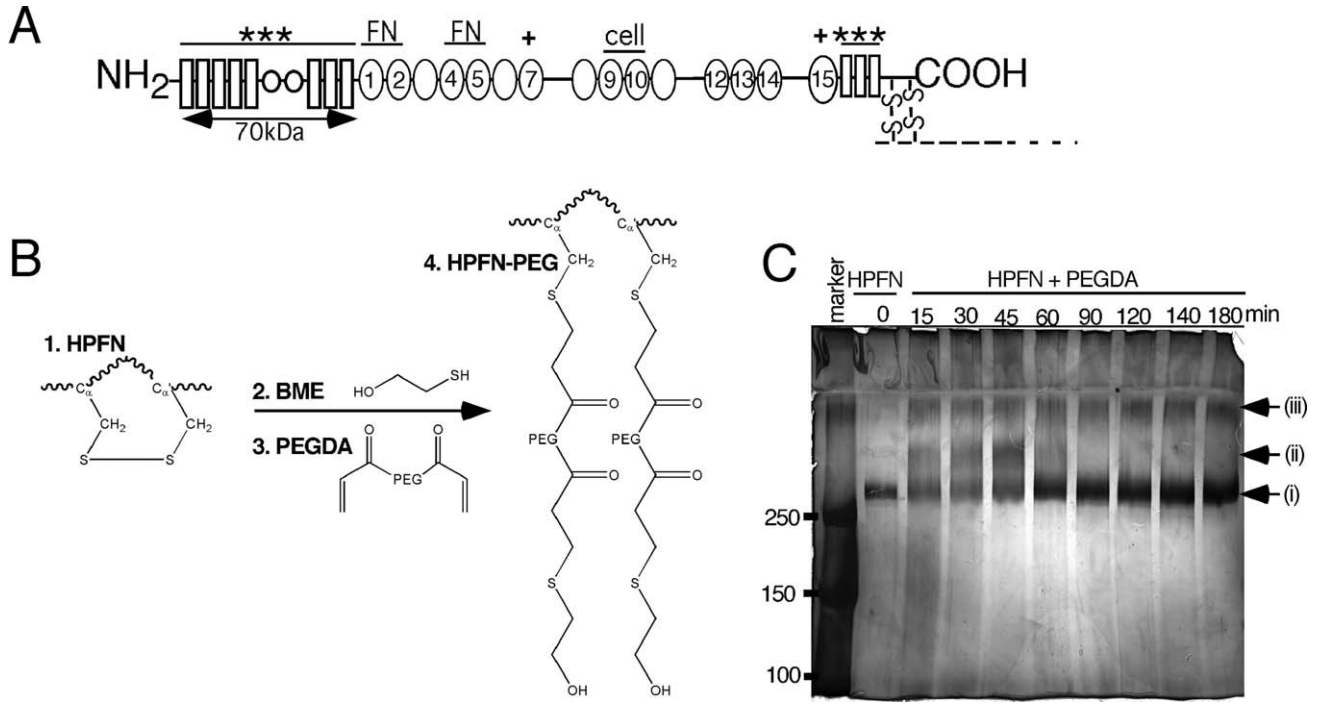

Figure 1. HPFN PEGylation.

(A) Domain structure of a monomer of HPFN showing type I, II, and III repeats as rectangles, circles and ovals respectively. Intramolecular disulfide bridges (***) are found in the 70 kDa amino-terminal and in the carboxy-terminal type I repeats as well as in the dimerization domain (-S-S-). Free sulfhydryls (+) are found in the hydrophobic core of III_7 and III_{15}. Binding sites for cells and FN are shown on top. (B) Scheme for the PEGylation of HPFN **1**. BME **2** was used to disrupt disulfide bonds exposing them for conjugation with PEGDA **3**. Unreacted acrylate groups were quenched with excess BME **2**. (C) SDS-PAGE and silver staining characterization of reduced HPFN and the products of HPFN PEGylation at different time points. The molecular weight markers in kDa are shown on left. Molecular weight of Bands (i), (ii), and (iii) is presented in Table 1.

repeats also harbor binding sites for cell adhesion receptors,[16,17] other FN molecules[27–31] and growth factors.[32,33] These responses are important in wound healing. Therefore, PEGylating on cysteine residues leaves the type III repeats unperturbed. We found that PEGylated HPFN was more proteolytically stable than native HPFN in the presence of α chymotrypsin or neutrophil elastase. PEGylated HPFN coated on surfaces supported cell attachment and spreading, cell migration and focal adhesion formation in a comparable manner to native HPFN similarly treated. The findings with respect to adhesion and focal adhesion formation were demonstrated in NIH 3T3 mouse fibroblasts as well as in human dermal fibroblasts. Interestingly, PEGylated HPFN was assembled into an ECM by mouse fibroblasts when present in its soluble form but not when coated on a surface. HPFN, on the other hand, was assembled into an ECM when coated on surfaces or in the culture medium. These novel findings present an approach by which HPFN can be modified to be proteolytically stable, without perturbing its ability to bind cells and other FN molecules.

Materials and Methods

Purification of HPFN

HPFN was isolated from frozen human plasma obtained from the blood bank at Rush Hospital. Human plasma was thawed at 37°C, centrifuged to remove residual cells and precipitates, and then passed through an agarose sepharose 4B column (Sigma-Aldrich, St Louis, MO). The sepharose column flow-through was passed through a column packed with gelatin agarose beads (GE Healthcare Biosciences, Pittsburgh, PA). The gelatin column was washed with phosphate buffered saline (PBS, Fisher Scientific, Pittsburgh, PA). Bound HPFN was eluted with 6 M urea in PBS. The optical density of HPFN at 280 nm was used to determine its concentration. The molecular weight of HPFN was characterized through sodium dodecyl sulfate polyacrylamide gel electrophoresis (SDS-PAGE) and silver staining. The yield of HPFN was approximately 30 mg of protein for 150 mL of human plasma. HPFN was dialyzed at 4°C overnight in PBS before the studies described below were conducted.

Synthesis and characterization of PEGylated HPFN

The procedure of Elbert et al.[34] was used to convert 3.35 kDa PEG (Sigma-Aldrich) to PEGDA for HPFN conjugation. The hydroxyl groups in PEG were reacted with acryloyl chloride (Sigma-Aldrich) to form terminal acrylates. The acrylation of PEG was confirmed by the presence of characteristic acrylate peaks at 5.8, 6.1, and 6.4 ppm in 1^H NMR ($CDCl_3$) spectra in an Avance Bruker model AQS 300 MHz spectrometer (Bruker BioSpin Corporation, Billerica, MA). Conjugation of PEGDA to HPFN was done through a Michael reaction as shown in Figure 1B. First, **[1]** or HPFN at a concentration of 90 μg/mL was mixed with **[2]**, β-mercaptoethanol (BME, Sigma-Aldrich), and incubated for 15 min at 37°C. The molar ratio of HPFN to BME was 1:10,000. Then an equal volume of **[3],** 4% (w/v) PEGDA solution, was added to the mixture of BME and HPFN. The solution was then incubated for 15 min to 3 h at 37°C. The final concentration of HPFN and PEGDA was 45 μg/mL and 2%

(w/v), respectively and the molar ratio of HPFN to PEGDA used was 1:33,000.

The extent of PEGylation was monitored by carrying out SDS-PAGE analysis of the aliquots of the reaction mixture at different time points. These were collected, placed on ice, mixed with a reducing electrophoresis buffer, and electrophoresed in a 7% polyacrylamide gel. The reducing electrophoresis buffer contained 6.6% (w/v) sodium dodecyl sulfate (SDS, Fischer Scientific), 33% (v/v) glycerol (Fisher Scientific) and 0.33 M Dithiothreitol (DTT, Sigma-Aldrich). The volume ratio of sample to the reducing electrophoresis buffer was 3:1. The proteins in the gels were visualized by silver staining after electrophoresis. The gels were imaged in a Chemidoc XRS imaging system (Biorad, Hercules, CA) and Quantity One software (Biorad) was used for densitometric analysis. For functional assays of cell adhesion and FN fibril formation, HPFN was PEGylated for an hour, placed on ice, mixed with 1 mM BME to quench the acrylate groups and dialyzed against PBS overnight at 4°C to remove unbound PEGDA and BME. Hydrolysis between PEGDA and proteins is a function of temperature and pH. The half-life of the bond between PEGDA and protein at 37°C is 3.5 days.[34] The hydrolysis of PEG was minimized by conducting subsequent experiments with PEGylated HPFN immediately after dialysis.

Proteolysis of PEGylated HPFN

The proteolysis of PEGylated HPFN was carried out using TLCK treated α chymotrypsin from bovine pancreas (Sigma-Aldrich) or recombinant human neutrophil elastase (Innovative Research, Novi, MI). Each protease was added to 40 μg/mL PEGylated HPFN or 40 μg/mL HPFN in PBS and incubated at room temperature for 30 min. The total volume was 1 mL. The mass ratio of α chymotrypsin to HPFN was 1:25 and that of neutrophil elastase to HPFN was 1:360. A 100 μL volume of the reaction mixture was sampled before α chymotrypsin addition and at 2.5, 5, 7.5, 10, 12.5, 15, 17.5, 20, and 30 min after the addition of α chymotrypsin. Similarly, a sample was collected before and after 1, 2.5, 5, 7.5, 10 15, and 30 min the addition of neutrophil elastase. Proteolysis at specific time points was inhibited by the addition of 2 mM phenylmethylsulfonyl fluoride (PMSF, Fisher Scientific). Each aliquot was mixed with a reducing electrophoresis buffer, boiled and then electrophoresed on a 7% SDS-PAGE gel. The products of proteolysis of HPFN and PEGylated HPFN were visualized after electrophoresis by silver staining. The gels were imaged and densitometric analysis was conducted to determine the amount of intact protein present at different time points.

Cell culture

Mouse embryonic fibroblasts, NIH 3T3 fibroblasts (ATCC, Manassas, VA) were cultured in Dulbecco's Modified Eagle's Medium (DMEM, Fisher Scientific) supplemented with 10% bovine calf serum (Fisher Scientific) at 37°C with 5% CO_2. NIH 3T3 fibroblast passages 13–18 were used for this study. The cells were grown to 80–90% confluency in 10 cm dishes.

Static adhesion assay

Glass coverslips were washed twice with 70% ethanol (Fisher Scientific) and twice in PBS. They were then incubated for 1 h at 37°C with either 40 μg/mL HPFN, 40 μg/mL PEGylated HPFN, 2% (w/v) PEGDA or PBS. The glass coverslips were rinsed twice with PBS then incubated with 1% (w/v) bovine serum albumin (BSA, Sigma-Aldrich) in PBS for 30 min at 37°C. They were then rinsed with PBS twice. NIH 3T3 fibroblast cells were trypsinized with 1 mg/mL of TPCK trypsin (Fisher Scientific) for 5 min at room temperature. TPCK trypsin was in 0.01% ethylenediaminetetracetic acid (EDTA, Fisher Scientific) in PBS. Trypsin was inactivated by adding 0.5 mg/mL soybean trypsin inhibitor (SBTI, Fisher Scientific) in PBS. The cells were isolated by centrifugation then resuspended in serum free DMEM solution. They were then added to the coated glass coverslips and incubated for 1 h at 37°C in 5% CO_2. A cell density of 4×10^4 cells per well was used. After incubation, the samples were washed twice with PBS, fixed with 3.7% (w/v) paraformaldehyde (Fisher Scientific) in PBS for 15 min. The cells were then washed twice with PBS and permeabilized with 0.5% NP-40 (Fisher Scientific) in PBS in 15 min. The samples were then washed twice with PBS and stained with fluorescein conjugated phalloidin (Invitrogen, Carlsbad, CA) and Hoechst 33258 (Fisher Scientific) in 2% (w/v) ovalbumin in PBS (Sigma-Aldrich) at a dilution of 1:50 and a concentration of 1 μg/mL respectively. Staining was carried out at 37°C for 45 min. The samples were washed three times with PBS followed by a last wash with deionized water and then mounted for microscopy using prolong antifade (Invitrogen, Carlsbad, CA).

Focal adhesion assays

Glass coverslips were placed in a 24-well plate incubated with 40 μg/mL PEGylated or native HPFN in PBS, 2% (w/v) PEGDA or PBS at 37°C. After 1 h, the coverslips were washed with PBS and incubated with 1% (w/v) BSA in PBS for 30 min. The coverslips were then washed twice with PBS and incubated with NIH 3T3 fibroblasts at a density of 2×10^4 cells per well in complete culture media. Cells were incubated on the coverslips for 6 h. After incubation, the coverslips were washed twice with PBS and then adherent cells were fixed by incubating them with 3.7% (w/v) paraformaldehyde in PBS. The coverslips were washed and then permeabilized by incubating them with 0.5% NP-40 in PBS. After washing in PBS, the cells were stained for vinculin by incubating them with monoclonal anti-vinculin antibody mouse IgG1 isotype (clone hVIN-1, Sigma-Aldrich). The antibody was used at a dilution of 1:200 in 2% (w/v) ovalbumin in PBS and incubation was carried out for 30 min at 37°C. After incubation with the primary antibody, the cells were washed with PBS and incubated for 30 min at 37°C with goat anti-mouse IgG (H+L) fluorescein conjugate (Invitrogen). The secondary antibody was used at a dilution of 1:600 in 2% (w/v) ovalbumin. The coverslips were then washed twice in PBS and once in deionized water. They were then mounted with ProLong Gold Antifade reagent and imaged.

In vitro wound healing ("scratch") assay

Glass coverslips were coated with 45 μg/mL of PEGylated or native HPFN in PBS. The controls consisted of uncoated glass coverslips or coverslips coated with 2% (w/v) PEGDA. Three coverslips were used for each treatment. The coverslips were then blocked with 1% (w/v) BSA in PBS for

30 min and then washed three times with PBS. NIH 3T3 mouse fibroblasts were plated at a density of 2×10^5 cells per mL in complete media, so that they became 80–90% confluent in 18 h. Scratches were then made on the cell monolayer with a 200 μL pipette tip. After scratching, the cell monolayer was washed with PBS to remove cell debris and then incubated with serum free media. Images of the area surrounding the scratch were taken at 2, 4, 6, and 9 h after incubation. The migration of the cells was determined from the images taken by using ImageJ software to measure of the distance which the cells at the edge of moving boundary covered at specific time points.

Assembly of exogenous HPFN into the ECM

Studies were conducted to compare the assembly of HPFN and PEGylated HPFN into fibrils in the ECM when the molecules were (i) coated on surfaces and (ii) present in the culture media. For coating studies, glass coverslips in a 24-well plate were incubated with 40 μg/mL of PEGylated or native HPFN overnight at 4°C. Control treatments consisted of glass coverslips incubated with 2% (w/v) PEGDA in PBS or PBS alone. The coated surfaces were washed twice with PBS and incubated with 2×10^5 cells per well for 24 h. The cells were maintained in complete culture media. The coverslips were then washed twice with PBS, fixed in 3.7 paraformaldehyde in PBS then washed in PBS. To visualize cell nuclei and HPFN fibrils the coverslips were first labeled with Hoechst 33258 and 7.1 mouse monoclonal antibodies (Developmental Studies Hybridoma Bank, Iowa city, IA). The stains were in 2% (w/v) ovalbumin in PBS. The concentration of Hoechst 33258 was 1 μg/mL and 7.1 antibodies were used at a dilution of 1:100. The samples were then washed twice with PBS and labeled with a secondary antibody, goat anti-mouse IgG (H+L) fluorescein conjugates. The secondary antibody was used at a dilution of 1:600 as in 2% (w/v) ovalbumin. Labeling was carried out for a further 30 min at 37°C. The samples were then washed three times with PBS and once with water. They were then mounted for microscopy using Prolong Gold antifade (Invitrogen).

The incorporation of soluble exogenous HPFN or PEGylated HPFN into fibrils in the ECM was conducted as follows. Rat plasma FN was obtained from gelatin affinity chromatography of rat plasma (Lampire Biologicals, Pipersville, PA) and used to coat glass coverslips to facilitate cell adhesion. The coating solution was 15 μg/mL of rat plasma FN in PBS. Coating was carried out for 30 min at 37°C. The surfaces were washed twice with PBS. NIH 3T3 mouse fibroblasts were added at a density of 2×10^5 cells per well. The cells were cultured in FN depleted medium, which was supplemented with either 40 μg of PEGylated or native HPFN. FN was effectively depleted from the culture media by gelatin affinity chromatography. The controls consisted of FN depleted culture media and FN depleted culture media supplemented with 20 mg of PEGDA. The cells were cultured for 24 h then fixed and stained for HPFN and cell nuclei as previously described.

Fluorescence microscopy and image analysis

Imaging was conducted as follows: (1) Images of fluorescein and Hoechst stains from the adhesion assay were collected using a Carl Zeiss Axiovert 40CL microscope coupled to an Axiocam ICM (Carl Zeiss Microscopy, LLC, Thornwood, New York). Images were analyzed by using ImageJ software (National Institutes of Health). The number of positively Hoechst stained nuclei in a 10× field was used to characterize cell attachment. The area of fluorescein stained cytoskeleton at 20× magnification was used to quantify cell spreading. Cell area was converted from pixelated units to μm^2 by Axiovision scaling software (Carl Zeiss). (2) All focal adhesion images were obtained using the Zeiss LSM 5 Pascal confocal microscope (Carl Zeiss) with a 63× oil objective, a low pass filter of 505 nm and excitation at 488 nm. Pinhole size and detector gain were maintained constant when imaging all treatment types. (3) Focal adhesions were identified as structures with a size of 1 μm and above. Focal adhesions were counted for 20 cells of each coverslip treatment type. (4) Fluorescence microcopy of HPFN in the ECM, was conducted using a Carl Zeiss Axiovert 40CL microscope with a fluorescein filter at 20× and 40× magnification. Exposure times were kept constant when examining different treatments.

Statistical analysis and data treatment

All the experiments were conducted three times with at least two replications per treatment. Four randomly selected regions per treatment were imaged and used to determine cell attachment. This resulted in a data set of 12 measurements for each treatment in an experiment. For the analysis of cell spreading, 60 randomly selected cells from each treatment were analyzed. A one-factor analysis of variance was used to statistically evaluate the effect of each treatment on cell attachment and spreading. A two-sided significance level of 5% was used for student's *t*-tests when comparing the means of the treatments. *P*-values less than or equal to 0.05 were considered statistically significant. Similar analyses were conducted for focal adhesion formation and cell migration.

Results

PEGylation of HPFN

PEG was activated for protein binding by converting it to PEGDA. We chose to use bifunctional PEGDA due to ease of synthesis and characterization. The yield of acrylate conversion obtained from ^1H NMR spectra of PEGDA was 93%. This is comparable to yields reported by others.[35–37] PEGylation was conducted by Michael reaction, which preferentially binds the acrylate ends of PEGDA macromers to thiols in cysteine residues. Cysteine residues make up 2.6% of the total amino acid residues in HPFN. Most of the cysteines in HPFN are located in the 70 kDa amino-terminal fragment (Figure 1A). With the exception of two cysteines in the type III repeats,[26] all the cysteines in HPFN are involved in intramolecular or intermolecular disulfide bonds. From the domain structure and amino acid sequence of HPFN obtained from the UniProtKB/Swiss-Prot database (UniProtKB/Swiss-Prot: P02751.4), we estimated that the type III repeats comprise 70% of HPFN by mass. Thus, a strategy that conjugates PEGDA to cysteine residues located at the ends of HPFN would leave a major functional part of HPFN unperturbed.

HPFN was PEGylated by a two-step process involving incubation with BME to disrupt disulfide bonds, followed by incubation with PEGDA (Figure 1B). The incubation with

Table 1. Molecular Weight Distribution of the Products of HPFN PEGylation: (A) before and (B) 45 min After the Addition of PEGDA to Reduced HPFN

Treatment	Band Position	Molecular Weight (kDa)	
		Average	Range
(A) Before PEGDA	(i)	272	264–288
(B) After PEGDA	(i)	288	264–308
	(ii)	488	409–495
	(iii)	2044	861–3.92 × 10^3

BME was carried out at 37°C for 15 min. The products of the second incubation were treated with a reducing electrophoresis buffer and resolved in a polyacrylamide gel. DTT in the reducing electrophoresis buffer quenched unreacted acrylate groups and reduced disulfide bonds. Figure 1C shows the gel resulting from electrophoresis before the addition of PEGDA to HPFN, and at different time points after the addition of PEGDA to HPFN. The markers in Figure 1C were used to generate a plot of logarithm of molecular weight versus distance migrated. From this plot, the molecular weight of HPFN and the products of HPFN PEGylation at different time points were determined. Table 1 shows the molecular weight of HPFN prior to the addition of PEGDA and 45 min after the addition of PEGDA. During PEGylation Band (i) in Figure 1C, became thicker and more intense with time. The range of molecular weight associated with this band changed from 264 to 288 kDa before PEGDA addition to 264–308 kDa, 45 min after incubation with PEGDA (Table 1). The average molecular weight of HPFN (Band (i) in Figure 1C) increased from 272 to 288 kDa, 45 min after the addition of PEGDA to HPFN. The increase in molecular weight of HPFN corresponds to the conjugation of up to 10 PEGDA molecules per monomer of HPFN. The range in molecular weight of PEGylated HPFN is consistent with HPFN being tethered to different amounts of PEGDA molecules.

The appearance of a band with an average molecular weight of 488 kDa after the addition of PEGDA was observed [Figure 1C, Band (ii)]. We also observed an accumulation of products with bands close to the boundary between the stacking and resolving gels [Figure 1C, Band (iii)]. The 488 kDa band disappeared after 60 min. It is unlikely that Band (ii) in Figure 1C consists of dimeric HPFN due to its size. It is more likely that it corresponds to the conjugation of approximately sixty molecules of PEG to a HPFN monomer. The protein sequence of human FN has at least 63 cysteines (UniProtKB/Swiss-Prot: P02751.4). Band (iii) in Figure 1C has a molecular weight of over 2,000 kDa (Table 1) and may consist of multiple HPFN molecules covalently linked to each other by bifunctional PEGDA molecules. The most abundant product of HPFN PEGylation, based on band intensity, was associated with the 288 kDa band (Figure 1C, Band (i)). Accumulation of the 288 kDa band reached steady state after 60 min. We, therefore, chose to examine the activity of PEGylated HPFN conjugates at the 60-min time point.

The products of HPFN PEGylation after 60 min were quenched with BME and dialyzed in PBS prior to functional analysis. Attempts to quantify the concentration of PEGylated HPFN conjugates by BCA analysis, optical density or silver staining resulted in higher than expected protein concentration, which were attributed to the tethered PEGDA. The concentration of PEGylated HPFN was matched to that of HPFN by conducting parallel studies with HPFN where PBS buffer was used instead of PEGDA during conjugation. As PEGylated HPFN conjugates did not precipitate from solution after centrifugation at high speed, the molar amount of soluble PEGylated HPFN and HPFN were comparable. The concentration of HPFN after dialysis was determined by optical density and BCA assays, and was then matched to the concentration of PEGylated HPFN. Hydrolysis of the ester bond between PEG and HPFN has been reported to take place over several days at 37°C.[34] Therefore, the studies to assess the stability and activity of PEGylated HPFN outlined below were conducted immediately after dialysis of PEGylated HPFN.

Proteolytic cleavage of PEGylated HPFN by α-chymotrypsin

The proteolytic stability of PEGylated HPFN in the presence of α chymotrypsin or neutrophil elastase was measured. Figures 2A,B show SDS-PAGE gels of PEGylated HPFN and HPFN at different time points after the addition of α chymotrypsin. There were fewer cleaved protein fragments in the gel for PEGylated HPFN (Figure 2A) than for HPFN (Figure 2B). Additionally, the amount of intact PEGylated HPFN underwent a significantly smaller time dependent change than the amount intact HPFN. Figure 2C shows the quantity of intact PEGylated HPFN or HPFN at 0, 15, and 30 min after protease addition. The data in Figure 2C was obtained from densitometric analyses of silver stained polyacrylamide gels. Thirty minutes after protease addition the proportion of intact protein, relative to the zero time point, was 56 and 90% for HPFN and PEGylated HPFN, respectively. PEGylated HPFN was also more proteolytically stable in the presence of neutrophil elastase than native HPFN (Figures 2D–F). Clearly, PEGylation of HPFN inhibits the degradation of HPFN by α chymotrypsin and neutrophil elastase.

Modulation of cell adhesion by PEGylated HPFN

We studied the functionality of PEGylated HPFN by conducting adhesion assays. We compared the adhesive response of NIH 3T3 mouse fibroblasts on surfaces coated with PEGylated HPFN to the response on HPFN coated surfaces in serum free media. The serum free environment was necessary in the adhesion assays to eliminate the contribution of growth factors and other ECM proteins present in serum on cell adhesion. Glass surfaces were coated with PEGylated HPFN or HPFN, then cell adhesion assays were conducted on the coated surfaces. PEGDA and uncoated glass surfaces were used as controls. Fluorescence microscopy of adherent cells demonstrated that mouse fibroblasts had robust cell attachment and spreading on surfaces coated with the PEGylated HPFN and native HPFN (Figure 3A). Cells attached on uncoated glass surfaces or surfaces coated with PEGDA. However, these cells had poor spreading when compared to cells on HPFN or PEGylated HPFN coated coverslips (Figure 3A). Quantitative analysis of cell attachment showed significantly greater cell attachment (Figure 3B) and spreading (Figure 3C) in cells cultured on surfaces treated with either PEGylated or native HPFN compared to cells cultured on untreated surfaces or surfaces coated with PEGDA. There was no significant difference in cell attachment or cell spreading between surfaces coated with PEGylated HPFN compared to native HPFN. Similar findings were obtained with the use of human dermal fibroblasts indicating that this

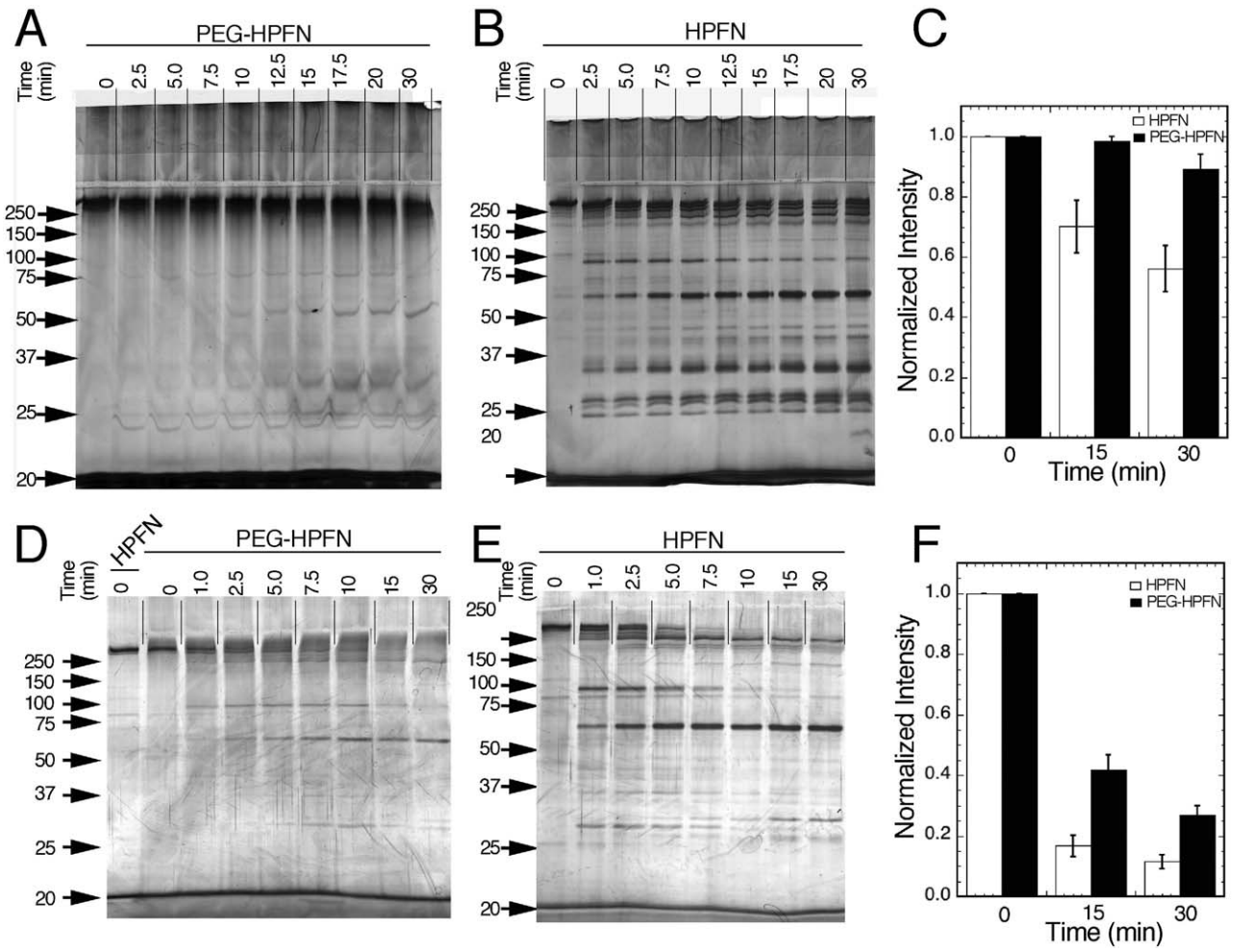

Figure 2. Effects of proteolysis of PEGylated and native HPFN.

HPFN was PEGylated for 60 min, then dialyzed overnight to remove unbound BME and PEGDA. α chymotrypsin (A, B, and C) or neutrophil elastase (D, E, and F) was added to native and PEGylated HPFN. SDS-PAGE analysis of the products of α chymotrypsin (A and B) and neutrophil elastase (D, E) cleavage at different time points. (C and F) Densitometric quantification of intact HPFN and PEGylated HPFN at zero, 15 and 30 min time points. The data has been normalized by dividing the band volume obtained with the zero time point. Error bars represent the range of two replicates.

observation was not specific to mouse fibroblasts (Supporting Information Figure S1). Therefore, conjugation of PEG to HPFN did not perturb its ability to mediate cell adhesion.

Formation of focal adhesions on glass coated with PEGylated HPFN

The engagement of adhesion receptors with FN coated on surfaces is followed by clustering of proteins such as vinculin into structures known as focal adhesions. We investigated whether vinculin was localized in focal adhesions of NIH 3T3 mouse fibroblasts by immunofluorescence microscopy. Focal adhesions were identified as aggregates with a size of 1 μm or larger. Figure 4A shows that there were numerous focal adhesions in cells cultured on surfaces coated with PEGylated and native HPFN after 6 h. Qualitatively, cells cultured on control PEGDA coated surfaces as well as glass surfaces had fewer and shorter focal adhesions. The number of focal adhesions per cell was comparable for PEGylated and native HPFN (Figure 4B). The same observations were made with human dermal fibroblasts (Supporting Information Figure S2). Hence, PEGylation of HPFN did not significantly perturb its ability to mediate focal adhesion formation on coated glass surfaces.

Cell migration on surfaces coated with PEGylated HPFN

Migration of fibroblasts into the wound bed is important for wound healing. We conducted in vitro scratch wound assays on fibroblasts cultured on glass surfaces coated with HPFN, PEG-HPFN or PEGDA. Cell culture was conducted in complete media and the migration assays were carried out in serum free media. After the creation of the scratch on the cell layer, we observed that the moving front formed "fingers" that reached out and migrated over the cell free surface (Figure 5A). The distance between "fingers" at opposite ends of the scratch was used to quantify migration over a period of 9 h. Two hours after the formation of a scratch on the cell layer, migration over glass surfaces coated with PEGylated or native HPFN was significantly higher than on surfaces coated with PEGDA (Figure 5B). This is inline with the observation of poor cell attachment on surfaces coated with PEGDA. Six and nine hours after the formation of a scratch on the cell layer, cells on the PEGylated and native HPFN migrated a longer distance than cells on PEGDA coated surfaces but this difference was significant only at the 6 h time point. Collectively, the data demonstrate that PEGylation of HPFN does not perturb its ability to mediate fibroblast migration on two-dimensional surfaces.

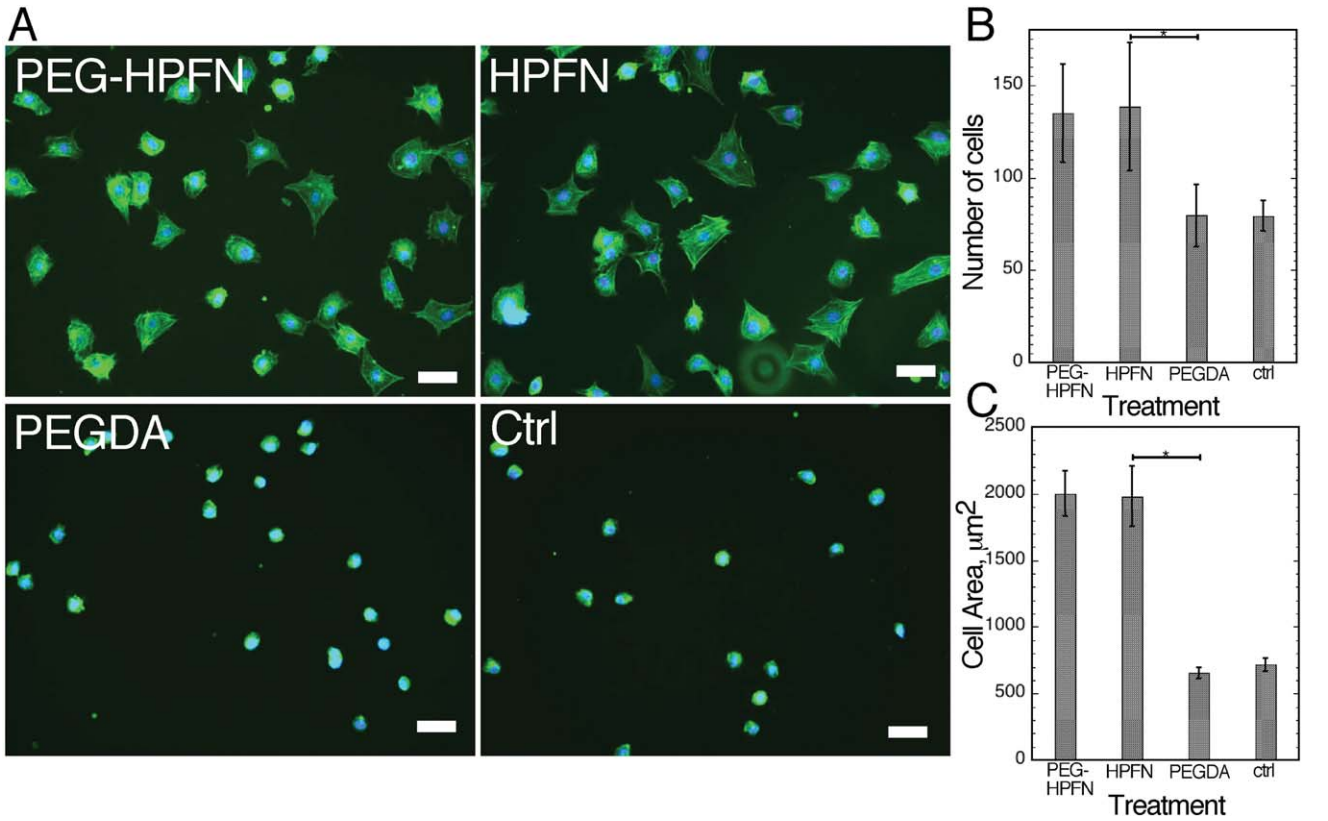

Figure 3. Adhesive response of NIH 3T3 mouse fibroblasts cultured on surfaces coated with HPFN, PEGylated HPFN and PEGDA.

(A) Cells were cultured in serum free media for an hour on glass surfaces incubated with PEGylated HPFN, HPFN, PEGDA and buffer (ctrl), then fixed and stained for nuclei (blue) and actin (green). Scale bar in A = 50 μm. Image analysis of: (B) the number of cells in a 10× objective and (C) cell area under a 20× objective. The data in both B and C represents the mean of two replicates and four fields per treatment. Sixty cells in C were analyzed. The error bars represent a 95% confidence interval of the standard error of the mean. "*" represents a statistically significant difference in the mean. [Color figure can be viewed in the online issue, which is available at wileyonlinelibrary.com]

The assembly of PEGylated HPFN conjugates into an ECM

FN is assembled by fibroblasts into ECM fibrils when immobilized on surfaces or when present in the culture media. Many cell types in culture, including mouse fibroblasts, can incorporate exogenous HPFN into their ECM. FN fibril formation in NIH 3T3 mouse fibroblasts cultured on surfaces coated with HPFN and PEGylated HPFN was characterized by immunofluorescence microscopy. Antibodies that bind specifically to HPFN were used to detect HPFN in the ECM. Glass surfaces coated with PEGDA as well as uncoated surfaces were used as negative controls. There were no HPFN fibrillar structures visualized in mouse fibroblasts cultured on surfaces coated with PEGylated HPFN (Figure 6A). However, fibroblasts organized HPFN coated on surfaces into fibrillar structures at the cell periphery (Figure 6B). Labeling of HPFN with the 7.1 antibodies was specific because the antibodies could detect the adsorbed HPFN in the background (insets of Figures 6A,B) but not on PEGDA coated or uncoated surfaces (Figure 6C,D). HPFN fibrils were not observed in cells cultured on uncoated surfaces or surfaces coated with PEGDA. PEGylation of HPFN inhibits its incorporation into ECM fibrils when it is coated on a surface.

We next examined the assembly of exogenous PEGylated HPFN in the culture media into ECM fibrils. Mouse fibroblasts were cultured in FN depleted media supplemented with HPFN or PEGylated HPFN for 24 h. Interestingly, supplemental PEGylated HPFN was assembled into ECM fibrils by mouse fibroblasts in a comparable manner to HPFN (Figures 7A,B). Fibroblasts cultured in FN depleted media or in FN depleted media supplemented with PEGDA did not positively stain for HPFN fibrils (Figures 7C,D). Thus, PEGylated HPFN mediates cell attachment and spreading, migration and focal adhesion formation. It is assembled into an ECM by mouse fibroblasts when present in the culture media, but not when coated on a surface.

Discussion

We present new evidence that PEGylation on reduced cysteines results in HPFN that is more proteolytically stable than native HPFN. This PEGylated HPFN supports cell adhesion, migration and focal adhesion formation in a comparable manner to HPFN. Furthermore, PEGylated HPFN in the culture media is assembled into ECM fibrils by mouse fibroblasts in a comparable manner to HPFN. Interestingly, HPFN and PEGylated HPFN differ in that native HPFN but not PEGylated HPFN coated to surfaces is assembled into ECM fibrils by adherent mouse fibroblasts. These new findings of FN stabilization demonstrate the potential of a therapeutic strategy that utilizes proteolytically stable and biologically active PEGylated HPFN in the chronic wound bed to stimulate biological responses associated with tissue repair.

The 70 kDa amino-terminal of HPFN was PEGylated on cysteines leaving two-thirds of HPFN unperturbed. The type

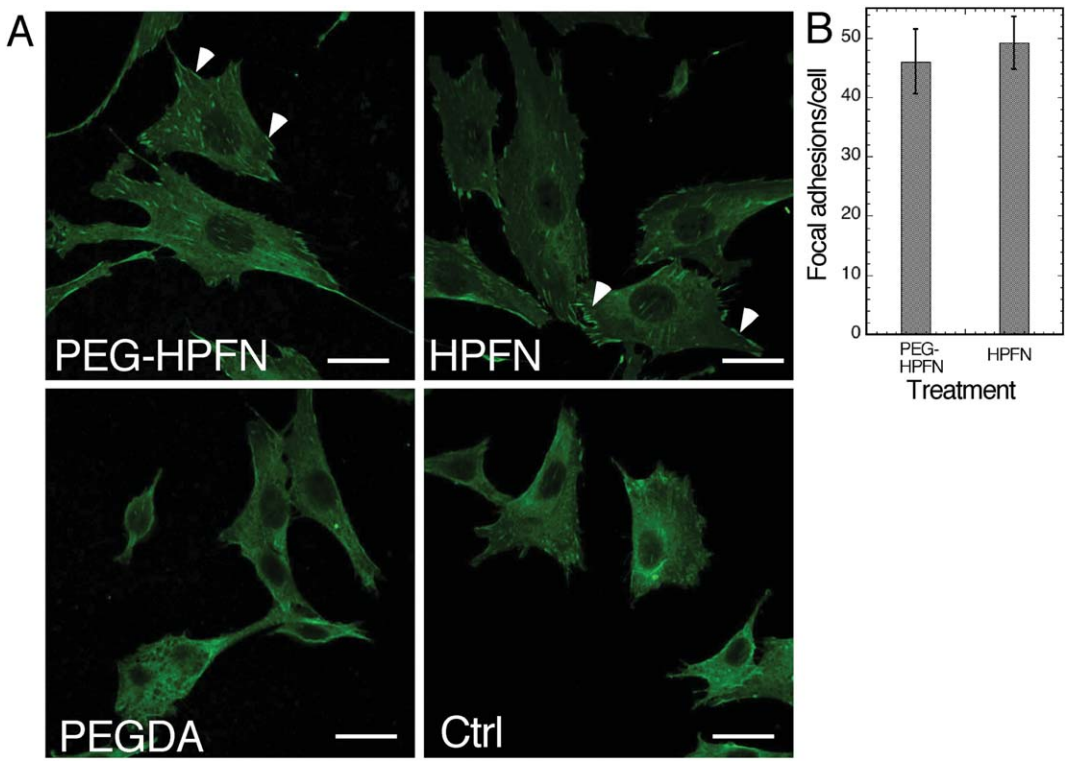

Figure 4. Focal adhesion formation by NIH 3T3 mouse fibroblasts on surfaces coated with PEGylated and native HPFN.

(A) Fluorescence microscopy images of vinculin staining in NIH 3T3 mouse fibroblasts after 6 h of culture on surfaces coated with PEGylated HPFN, HPFN and PEGDA as well as glass surfaces (ctrl). Arrows point to focal adhesions. (B) Number of focal adhesions per cell on native and PEGylated HPFN. Scale bar = 20 μm. [Color figure can be viewed in the online issue, which is available at wileyonlinelibrary.com]

III repeats of HPFN, form the bulk of the protein by mass and contain two free cysteines in the hydrophobic core of the repeats.[26,38] They also support cell adhesion in $III_{9–10}$ and FN binding in $III_{1–2}$, $III_{4–5}$, III_{10}, and $III_{12–14}$.[11,39,40] Thus, the 70 kDa amino-terminal but not the type III repeats are perturbed in our approach to PEGylate HPFN. Both human dermal fibroblasts and NIH 3T3 mouse fibroblasts adhere to FN.[41–45] Our finding that PEGylated HPFN is comparable to HPFN, with respect to modulation of cell adhesion in both cell types, demonstrates that the cell-binding domain in $III_{9–10}$ is functional after PEGylation. Moreover, studies have shown that when $III_{9–10}$ is coated on glass coverslips it elicits a comparable level of focal adhesion formation to that of FN coated surfaces.[45] Therefore, the functionality of $III_{9–10}$ after PEGylation is further supported by our demonstration that both mouse and human fibroblasts are able to form focal adhesions on both PEGylated and native HPFN. A similar argument can be made for fibroblast migration on FN. FN supports cell migration through interactions in $III_{9–10}$.[46–48] We observed comparable amount of cell migration on PEGylated and native HPFN, which we attribute to a biologically functional $III_{9–10}$. Interestingly, whereas

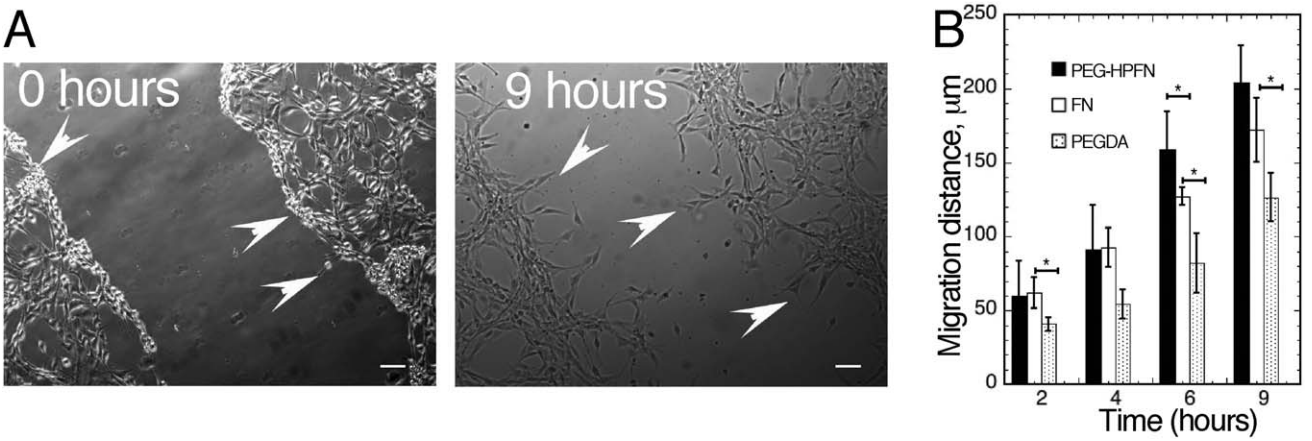

Figure 5. Cell migration on surfaces coated with PEGylated HPFN.

(A) Phase contrast images of NIH 3T3 fibroblasts on PEG-HPFN coated surfaces at 0 and 9 h after wounding. The moving front extended "fingers" into the cell free area (arrows). Scale bar = 100 μm. (B) The migration distance of cells in the "fingers" at both edges of the scratch were measured at 2, 4, 6, and 9 h on PEG-HPFN, HPFN or PEGDA coated glass surfaces. Values represent means ± standard error the mean of three independent experiments. "*" represents a statistically significant difference in the mean.

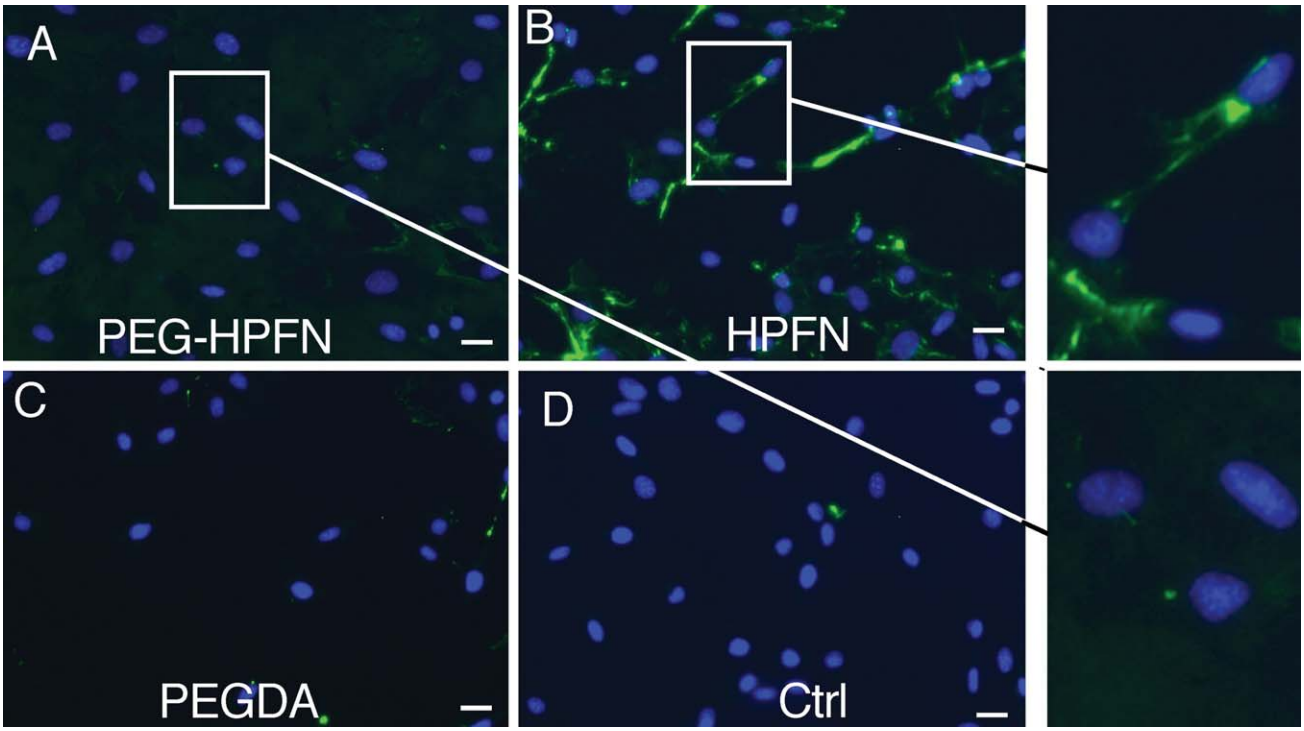

Figure 6. Assembly of PEGylated and native HPFN coated on glass surfaces into ECM fibrils.

NIH 3T3 mouse fibroblasts were cultured in complete media for 24 h on glass surfaces coated with PEGylated HPFN (A), native HPFN (B), PEGDA (C) or on uncoated surfaces (D). The cells were fixed and stained for with Hoechst for nuclei (blue) and with mouse monoclonal antibodies specific for HPFN followed by fluorescein goat anti-mouse polyclonal antibodies (green). Scale bar = 20 μm. [Color figure can be viewed in the online issue, which is available at wileyonlinelibrary.com]

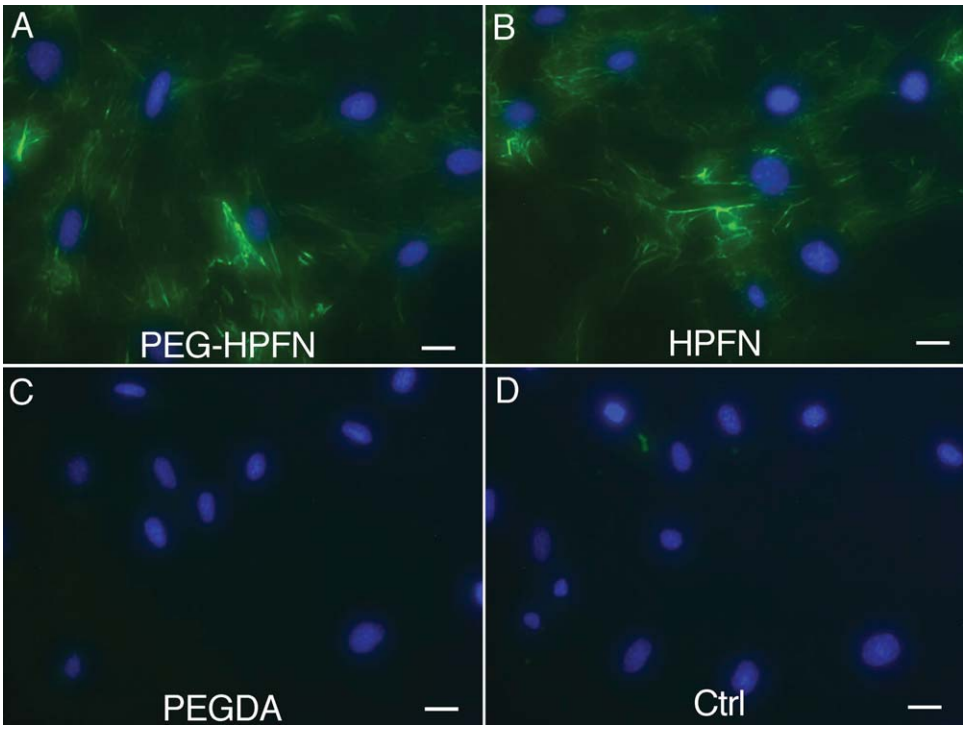

Figure 7. Assembly of soluble PEGylated and native HPFN into ECM fibrils.

Cells were cultured in HPFN depleted media supplemented with 40 μg of PEGylated human HPFN (A), 40 μg human HPFN (B), 20 mg PEGDA (C) or buffer (D) for 24 h. They were then fixed and stained for nuclei (blue) and with mouse monoclonal antibodies specific for HPFN followed by goat anti-mouse polyclonal antibodies (green). Scale bar = 20 μm. [Color figure can be viewed in the online issue, which is available at wileyonlinelibrary.com]

both soluble and immobilized HPFN are assembled into fibrils, soluble but not immobilized PEGylated HPFN is assembled into fibrils in the ECM. As the 70 kDa amino-terminal fragment forms binding interactions with a number of type III repeats when coated on glass surfaces,[31,49] it maybe that PEGylation on this site disrupts FN-FN interactions necessary for FN fibrillogenesis in the immobilized form of the molecule.

An alternative mechanism to describe differences in FN fibril formation between PEGylated and native HPFN coated on surfaces is based on the exposure of cryptic binding sites during fibrillogenesis. FN fibril formation is proposed to occur when hidden or cryptic FN binding sites are exposed by proteolysis or cell mediated extension.[11] Fibrillogenesis involving PEGylated HPFN coated on surfaces may favor proteolysis for exposure of FN binding sites. As PEGylated HPFN is more proteolytically stable than HPFN, then fibril formation by proteolytic processing is retarded. Conversely, fibril formation from soluble FN may favor cell-mediated extension over proteolytic cleavage for exposure of cryptic FN binding sites. As PEGylated HPFN binds cells to the same extent as HPFN, the exposure of cryptic FN binding sites by cell-mediated extension may activate fibril formation in the same manner in HPFN as in PEGylated HPFN. FN is secreted as a soluble molecule and converted to the fibrillar form by cells. Therefore, fibril assembly of soluble PEGylated HPFN is more biologically relevant than fibril formation on coated surfaces.

There is variability in FN structure and composition. FN undergoes alternative splicing which leads to several isoforms of the protein.[50–52] HPFN, compared to FN secreted by tissue cells in the wound bed or cellular FN, undergoes less splicing and is more homogenous.[38] In the wound bed, fibrillar FN in the ECM arises from both cells and plasma.[22–24] Fibrillar FN is more elongated compared to cellular FN.[53,54] We expect that PEGylation of cellular FN or fibrillar FN will result in proteolytic stability of FN in the wound bed ECM but may also result in additional biological responses to those examined here. For example, one of the alternatively spliced domains in FN, IIICS, is cryptic in FN but is exposed when FN is cleaved by proteases.[5,55] Subsequently, cleavage leads to exposure of binding sites for $\alpha_4\beta_1$ integrins which then modulate cell adhesion and FN production.[56,57] Thus, the choice of PEGylation of HPFN over cellular FN was due to the fact that it has less variability and was subsequently easier to study.

The wound environment is complex and it involves multiple players. By developing a simple model herein, we demonstrate how FN can be stabilized without perturbing its activity. Some of the simplifications made in this study are justified as follows: (1) The protease α chymotrypsin was selected due to ease of accessibility and because its cleavage of FN in solution has been demonstrated[49,58,59] and neutrophil elastase was selected because it is elevated in chronic wounds . Both α chymotrypsin and neutrophil elastase are members of the of serine proteases family of enzymes which are elevated in the chronic wound bed.[2,3] (2) HPFN was used because it is incorporated in the wound bed ECM[22–24] and is easy to isolate. (3) Fibroblasts are a relevant model system because during wound healing they migrate from the surrounding tissue, attach to the wound bed, and assemble an ECM.[15,60,61] (4) PEGDA was selected over PEG methacrylate for PEGylation due to ease of synthesis and characterization. Studies have shown that factors such as the site at which the PEG molecule is grafted to the protein, the chemistry of attachment, the size of the PEG molecule and branching in PEG may impact protein stability and function.[62,63] Given the numerous possibilities present, our strategy of targeting cysteine residues and leaving more than two-thirds of FN unperturbed, helps in narrowing the design space for future studies in this area.

Our study demonstrates that FN can be stabilized against proteolytic degradation by PEGylation and that PEGylated FN supports cell adhesion. We also show that PEGylated FN in culture media is assembled into FN fibrils. Our method provides an avenue by which systematic variation of PEGylation can be used to modulate proteolytic stability and functional activity. This will in turn open the door to therapeutic applications of stable and bioactive forms of FN in the chronic wound bed.

Acknowledgments

The authors like to thank Dr. Yu-Chieh Chiu, Dr. Eric Brey and Dr. Victor Perez-Luna for useful advice on PEGDA synthesis, Dr. Hyun-Soon Chong for access and use of NMR and Dr. Nick Menhart for help on acquisition of human plasma. The authors would also like to thank Dr. Eric Brey for use of the confocal microscope. This research is supported by start-up funds from IIT to Nancy W. Karuri.

Literature Cited

1. Nwomeh BC, Yager DR, Cohen IK. Physiology of the chronic wound. *Clin Plast Surg*. 1998;25:341–356.
2. Grinnell F, Zhu M. Identification of neutrophil elastase as the proteinase in burn wound fluid responsible for degradation of fibronectin. *J Invest Dermatol*. 1994;103 155–161.
3. Rao CN, Ladin DA, Liu YY, Chilukuri K, Hou ZZ, Woodley DT. Alpha 1-antitrypsin is degraded and non-functional in chronic wounds but intact and functional in acute wounds: the inhibitor protects fibronectin from degradation by chronic wound fluid enzymes. *J Invest Dermatol*. 1995;105:572–578.
4. Trengove NJ, Stacey MC, MacAuley S, Bennett N, Gibson J, Burslem F, Murphy G, Schultz G. Analysis of the acute and chronic wound environments: the role of proteases and their inhibitors. *Wound Repair Regen*. 1999;7:442–452.
5. Ugarova TP, Ljubimov AV, Deng L, Plow EF. Proteolysis regulates exposure of the IIICS-1 adhesive sequence in plasma fibronectin. *Biochemistry*. 1996;35:10913–10921.
6. Menke NB, Ward KR, Witten TM, Bonchev DG, Diegelmann RF. Impaired wound healing. *Clin Dermatol*. 2007;25:19–25.
7. Moor AN, Vachon DJ, Gould LJ. Proteolytic activity in wound fluids and tissues derived from chronic venous leg ulcers. *Wound Repair Regen*. 2009;17:832–839.
8. Wilgus TA. Immune cells in the healing skin wound: influential players at each stage of repair. *Pharmacol Res*. 2008;58:112–116.
9. Wysocki AB, Grinnell F. Fibronectin profiles in normal and chronic wound fluid. *Lab Invest*. 1990;63:825–831.
10. Clark RA. Potential roles of fibronectin in cutaneous wound repair. *Arch Dermatol*. 1988;124:201–206.
11. Singh P, Carraher C, Schwarzbauer JE. Assembly of Fibronectin Extracellular Matrix. *Annu Rev Cell Dev Biol*. 2010;26:397–419.
12. Kapila YL, Kapila S, Johnson PW. Fibronectin and fibronectin fragments modulate the expression of proteinases and proteinase inhibitors in human periodontal ligament cells. *Matrix Biol*. 1996;15:251–261.
13. Norris DA, Clark RA, Swigart LM, Huff JC, Weston WL, Howell SE. Fibronectin fragment(s) are chemotactic for human peripheral blood monocytes. *J Immunol*. 1982;129:1612–1618.
14. Shiota S, Takano K, Nakagawa H. A 10-kda fragment of fibronectin type III domain is a neutrophil chemoattractant purified

from conditioned medium of rat granulation tissue. *Biol Pharm Bull*. 2001;24:835–837.
15. Grinnell F. Fibronectin and wound healing. *J Cell Biochem*. 1984;26:107–116.
16. McDonald JA, Quade BJ, Broekelmann TJ, LaChance R, Forsman K, Hasegawa E, Akiyama S. Fibronectin's cell-adhesive domain and an amino-terminal matrix assembly domain participate in its assembly into fibroblast pericellular matrix. *J Biol Chem*. 1987;262:2957–2967.
17. Sechler JL, Rao H, Cumiskey AM, Vega-Colon I, Smith MS, Murata T, Schwarzbauer J E. A novel fibronectin binding site required for fibronectin fibril growth during matrix assembly. *J Cell Biol*. 2001;154:1081–1088.
18. Grinnell F, Feld M, Minter D. Fibroblast adhesion to fibrinogen and fibrin substrata: requirement for cold-insoluble globulin (plasma fibronectin). *Cell*. 1980;19:517–525.
19. Yang C, Lu D, Liu Z. How PEGylation enhances the stability and potency of insulin: a molecular dynamics simulation. *Biochemistry*. 2011;50:2585–2593.
20. Wang W. Instability, stabilization, and formulation of liquid protein pharmaceuticals. *Int J Pharm*. 1999;185:129–188.
21. Veronese FM, Mero A. The impact of PEGylation on biological therapies. *BioDrugs*. 2008;22:315–329.
22. Allen-Hoffmann BL, Crankshaw CL, Mosher DF. Transforming growth factor beta increases cell surface binding and assembly of exogenous (plasma) fibronectin by normal human fibroblasts. *Mol Cell Biol*. 1988;8:4234–4242.
23. Powanda MC, Moyer ED. Plasma proteins and wound healing. *Surg Gynecol ObstetI*. 1981;153:749–755.
24. To WS, Midwood KS. Plasma and cellular fibronectin: distinct and independent functions during tissue repair. *Fibrogenesis Tissue Repair*. 2011;4:21–38.
25. Balian G, Click EM, Crouch E, Davidson JM, Bornstein P. Isolation of a collagen-binding fragment from fibronectin and cold-insoluble globulin. *J Biol Chem*. 1979;254:1429–1432.
26. Lemmon CA, Ohashi T, Erickson HP. Probing the folded state of fibronectin type III domains in stretched fibrils by measuring buried cysteine accessibility. *J Biol Chem*. 2011;286:26375–26382.
27. Aguirre KM, McCormick RJ, Schwarzbauer JE. Fibronectin self-association is mediated by complementary sites within the amino-terminal one-third of the molecule. *J Biol Chem*. 1994; 269:27863–27868.
28. Hocking DC, Sottile J, McKeown-Longo PJ. Fibronectin's III-1 module contains a conformation-dependent binding site for the amino-terminal region of fibronectin. *J Biol Chem*. 1994; 269:19183–19187.
29. Maqueda A, Moyano JV, Hernandez Del Cerro M, Peters DM, Garcia-Pardo A. The heparin III-binding domain of fibronectin (III4-5 repeats) binds to fibronectin and inhibits fibronectin matrix assembly. *Matrix Biol*. 2007;26:642–651.
30. Hocking DC, Smith RK, McKeown-Longo PJ. A novel role for the integrin-binding III-10 module in fibronectin matrix assembly. *J Cell Biol*. 1996;133:431–444.
31. Bultmann H, Santas AJ, Peters DMP. Fibronectin fibrillogenesis involves the heparin II binding domain of fibronectin. *J Biol Chem*. 1998;273:2601–2609.
32. Millis AJT, Hoyle M, Mann DM, Brennan MJ. Incoporation of cellular and plasma fibronectin into smooth-muscle cell exreacellular-matrix invitro. *Proc Natl Acad Sci USA*. 1985; 82:2746–2750.
33. Martino MM. Hubbell JA. The 12th-14th type III repeats of fibronectin function as a highly promiscuous growth factor-binding domain. *FASEB J*. 2010;24:4711–4721.
34. Elbert DL, Hubbell JA. Conjugate addition reactions combined with free-radical cross-linking for the design of materials for tissue engineering. *Biomacromolecules*. 2001;2:430–441.
35. Cruise GM, Scharp DS, Hubbell JA. Characterization of permeability and network structure of interfacially photopolymerized poly(ethylene glycol) diacrylate hydrogels. *Biomaterials*. 1998;19:1287–1294.
36. Lutolf MP, Tirelli N, Cerritelli S, Cavalli L, Hubbell JA. Systematic modulation of Michael-type reactivity of thiols through the use of charged amino acids. *Bioconjug Chem*. 2001; 12:1051–1056.
37. Salinas CN, Anseth KS. Mixed mode thiol-acrylate photopolymerizations for the synthesis of PEG-peptide hydrogels. *Macromolecules*. 2008;41:6019–6026.
38. Pankov R, Yamada KM. Fibronectin at a glance. *J Cell Sci*. 2002;115:3861–3863.
39. Kshatriya PP, Karuri SW, Chiang C, Karuri, NW. A combinatorial approach for directing the amount of fibronectin fibrils assembled by cells that uses surfaces derivatized with mixtures of fibronectin and cell binding domains. *Biotechnol Progr*. 2012; 28: 862–871.
40. Chiang C, Karuri, SW, Kshatriya, PP, Schwartz, J, Schwarzbauer, J, Karuri, NW. A surface derivatization strategy for combinatorial analysis of cell response to mixtures of protein domains. *Langmuir*. 2012;28:548–556.
41. Balklava Z, Verderio E, Collighan R, Gross S, Adams J, Griffin M. Analysis of tissue transglutaminase function in the migration of swiss 3T3 fibroblasts - The active-state conformation of the enzyme does not affect cell motility but is important for its secretion. *J Biol Chem*. 2002;277:16567–16575.
42. Dalton SL, Scharf E, Briesewitz R, Marcantonio EE, Assoian RK. Cell-adhesion to extracellular-matrix regulates the life-cycle of integrins. *Mol Biol Cell*. 1995;6:1781–1791.
43. Hanks SK, Calalb MB, Harper MC, Patel SK. Focal adhesion protein-tyrosine kinase phosphorylated in response to cell attachment to fibronectin. *Proc Natl Acad Sci USA*. 1992;89:8487–8491.
44. Son HJ, Han DW, Kim HH, Kim HJ, Lee IS, Kim JK, Park JC. Attachment and proliferation of human dermal fibroblasts onto ECM-immobilized PLGA films. In: Zhang X, Tanaka J, Yu Y, Tabata Y. editors. *ASBM6: Advanced Biomaterials VI*. Zurich-Uetikon: Trans Tech Publications Ltd; 2005:288–289, 291–294.
45. Wang RX, Clark RAF, Mosher DF, Ren XD. Fibronectin's central cell-binding domain supports focal adhesion formation and rho signal transduction. *J Biol Chem*. 2005;280:28803–28810.
46. Seppa HE, Yamada KM, Seppa ST, Silver MH, Kleinman HK, Schiffmann E., The cell binding fragment of fibronectin is chemotactic for fibroblasts. *Cell Biol Int Rep*. 1981;5:813–819.
47. Postlethwaite AE, Keski-Oja J, Balian G, Kang AH., Induction of fibroblast chemotaxis by fibronectin. Localization of the chemotactic region to a 140,000-molecular weight non-gelatin-binding fragment. *J Exp Med*. 1981;153:494–499.
48. Alfandari D, Cousin H, Gaultier A, Hoffstrom BG, DeSimone DW. Integrin alpha5beta1 supports the migration of Xenopus cranial neural crest on fibronectin. *Dev Biol*. 2003;260:449–464.
49. Karuri NW, Lin Z, Rye HS, Schwarzbauer JE. Probing the conformation of the fibronectin III1-2 domain by fluorescence resonance energy transfer. *J Biol Chem*. 2009;284:3445–3452.
50. Burton-Wurster N, Gendelman R, Chen H, Gu DN, Tetreault JW, Lust G, Schwarzbauer JE, MacLeod JN. The cartilage-specific (V+C)- fibronectin isoform exists primarily in homodimeric and monomeric configurations. *Biochem J*. 1999;341 (Pt 3):555–561.
51. Schwarzbauer JE. Alternative splicing of fibronectin: three variants, three functions. *Bioessays*. 1991;13:527–533.
52. Tamkun JW, Schwarzbauer JE, Hynes RO. A single rat fibronectin gene generates three different mRNAs by alternative splicing of a complex exon. *Proc Natl Acad Sci USA*. 1984;81:5140–5144.
53. Ohashi T, Kiehart DP, Erickson HP. Dynamics and elasticity of the fibronectin matrix in living cell culture visualized by fibronectin-green fluorescent protein. *Proc Natl Acad Sci USA*. 1999;96:2153–2158.
54. Smith ML, Gourdon D, Little WC, Kubow KE, Eguiluz RA, Luna-Morris S, Vogel V. Force-induced unfolding of fibronectin in the extracellular matrix of living cells. *PLoS Biol*. 2007;5:e268.
55. Valenick LV, Hsia HC, Schwarzbauer JE. Fibronectin fragmentation promotes alpha4beta1 integrin-mediated contraction of a fibrin-fibronectin provisional matrix. *Exp Cell Res*. 2005;309:48–55.

56. Schwarzbauer JE, Spencer CS, Wilson CL. Selective secretion of alternatively spliced fibronectin variants. *J Cell Biol*. 1989;109:3445–3453.
57. Manabe R, Ohe N, Maeda T, Fukuda T, Sekiguchi K. Modulation of cell-adhesive activity of fibronectin by the alternatively spliced EDA segment. *J Cell Biol*. 1997;139:295–307.
58. Bernard BA, Yamada KM, Olden K. Carbohydrates selectively protect a specific domain of fibronectin against proteases. *J Biol Chem*. 1982;257:8549–8554.
59. Hahn LH, Yamada KM. Identification and isolation of a collagen-binding fragment of the adhesive glycoprotein fibronectin. *Proc Natl Acad Sci USA*. 1979;76:1160–1163.
60. Clark RA. Basics of cutaneous wound repair. *J Dermatol Surg Oncol*. 1993;19:693–706.
61. Stroncek JD, Bell N, Reichert WM. Instructional PowerPoint presentations for cutaneous wound healing and tissue response to sutures. *J Biomed Mater Res A*. 2009;90:1230–1238.
62. Grace MJ, Lee S, Bradshaw S, Chapman J, Spond J, Cox S, Delorenzo M, Brassard D, Wylie D, Cannon-Carlson S, Cullen C, Indelicato S, Voloch M, Bordens R. Site of pegylation and polyethylene glycol molecule size attenuate interferon-alpha antiviral and antiproliferative activities through the JAK/STAT signaling pathway. *J Biol Chem*. 2005;280:6327–6336.
63. Roberts MJ, Bentley MD, Harris JM. Chemistry for peptide and protein PEGylation. *Adv Drug Delivery Rev*. 2002;54:459–476.

Manuscript received Sep. 2, 2012, and revision received Nov. 26, 2012.